

1 **Not all feldspars are equal: a survey of ice nucleating**
2 **properties across the feldspar group of minerals**

3

4 **Alexander D. Harrison^{1‡}, Thomas F. Whale^{1**}, Michael A. Carpenter², Mark A.**
5 **Holden¹, Lesley Neve¹, Daniel O’Sullivan¹, Jesus Vergara Temprado¹, Benjamin**
6 **J. Murray^{1*}**

7 ¹School of Earth and Environment, University of Leeds, Leeds, LS2 9JT, UK

8 ² Department of Earth Sciences, University of Cambridge, Downing Street, Cambridge CB2
9 3EQ, UK

10 Correspondence to: T. F. Whale (t.f.whale@leeds.ac.uk) and B. J. Murray
11 (b.j.murray@leeds.ac.uk)

12

13 ‡ Both authors contributed equally to the paper

14

15 **Abstract**

16 Mineral dust particles from wind-blown soils are known to act as effective ice nucleating
17 particles in the atmosphere and are thought to play an important role in the glaciation of
18 mixed phase clouds. Recent work suggests that feldspars are the most efficient nucleators of
19 the minerals commonly present in atmospheric mineral dust. However, the feldspar group of
20 minerals is complex, encompassing a range of chemical compositions and crystal structures.
21 To further investigate the ice-nucleating properties of the feldspar group we measured the ice
22 nucleation activities of 15 characterised feldspar samples. We show that alkali feldspars, in
23 particular the potassium feldspars, generally nucleate ice more efficiently than feldspars in
24 the plagioclase series which contain significant amounts of calcium. We also find that there is
25 variability in ice nucleating ability within these groups. While five out of six potassium-rich
26 feldspars have a similar ice nucleating ability, one potassium rich feldspar sample and one
27 sodium-rich feldspar sample were significantly more active. The hyper-active Na-feldspar
28 was found to lose activity with time suspended in water with a decrease in mean freezing
29 temperature of about 16°C over 16 months; the mean freezing temperature of the hyper-
30 active K-feldspar decreased by 2°C over 16 months, whereas the ‘standard’ K-feldspar did

1 not change activity within the uncertainty of the experiment. These results, in combination
2 with a review of the available literature data, are consistent with the previous findings that
3 potassium feldspars are important components of arid or fertile soil dusts for ice nucleation.
4 However, we also show that there is the possibility that some alkali feldspars may have
5 enhanced ice nucleating abilities, which could have implications for prediction of ice
6 nucleating particle concentrations in the atmosphere.

7

8 **1 Introduction**

9 Clouds containing supercooled liquid water play an important role in our planet's climate and
10 hydrological cycle, but the formation of ice in these clouds remains poorly understood
11 (Hoose and Möhler, 2012). Cloud droplets can supercool to below -35°C in the absence of
12 particles capable of nucleating ice (Riechers et al., 2013; Herbert et al., 2015), hence clouds
13 are sensitive to the presence of ice nucleating particles (INPs). A variety of aerosol types
14 have been identified as INPs (Murray et al., 2012; Hoose and Möhler, 2012), but mineral
15 dusts from deserts are thought to be important INPs over much of the globe and in a variety
16 of cloud types (DeMott et al., 2003; Hoose et al., 2008; Hoose et al., 2010; Niemand et al.,
17 2012; Atkinson et al., 2013).

18 Atmospheric mineral dusts are composed of weathered mineral particles from rocks and soils,
19 and are predominantly emitted to the atmosphere in arid regions such as the Sahara (Ginoux
20 et al., 2012). The composition and relative concentrations of dust varies spatially and
21 temporally but it is generally made up of only a handful of dominant minerals. The most
22 common components of dust reflect the composition of the continental crust and soil cover,
23 with clay minerals, feldspars and quartz being major constituents. Until recently, major
24 emphasis for research has been placed on the most common minerals in transported
25 atmospheric dusts, the clays. It has now been shown that, when immersed in water, the
26 feldspar component nucleates ice much more efficiently than the other main minerals that
27 make up typical desert dust (Atkinson et al., 2013; Augustin-Bauditz et al., 2014; O'Sullivan et
28 al., 2014; Niedermeier et al., 2015; Zolles et al., 2015). This is an important finding as it has
29 been demonstrated that feldspar is a common component of aerosolised mineral dusts
30 (Glaccum and Prospero, 1980; Kandler et al., 2009; Kandler et al., 2011; Atkinson et al.,
31 2013; Perlwitz et al., 2015). Feldspar particles in the atmosphere tend to be larger than clay
32 particles and so will have shorter lifetimes in the atmosphere, however aerosol modelling

1 work has suggested that feldspar particles can account for many observations of INP
2 concentrations around the world (Atkinson et al., 2013). Work conducted below water
3 saturation using a continuous flow diffusion chamber has also concluded that feldspars,
4 particularly orthoclase feldspars, nucleate ice at lower relative humidity in the deposition
5 mode than other common dust minerals (Yakobi-Hancock et al., 2013). While all available
6 evidence indicates that feldspars are very effective INPs, it must also be recognised that
7 feldspars are a group of minerals with differing compositions and crystal structures.
8 Therefore, in this study we examine immersion mode ice nucleation by a range of feldspar
9 samples under conditions pertinent to mixed phase clouds.

10 An additional motivation is that determining the nature of nucleation sites is of significant
11 fundamental mechanistic interest and is likely to help with further understanding of ice
12 nucleation in the atmosphere (Vali, 2014; Freedman, 2015; Slater et al., 2015). By
13 characterising a range of feldspars and associating them with differences in ice nucleation
14 activity it might be possible to build understanding of the ice nucleation sites on feldspars.
15 Some work has been conducted in this area already. Augustin-Bauditz et al. (2014) concluded
16 that microcline nucleates ice more efficiently than orthoclase on the basis of ice nucleation
17 results looking at a microcline feldspar and several mixed dusts. Zolles et al. (2015) recently
18 found that a plagioclase and an albite feldspar nucleated ice less well than a potassium
19 feldspar and suggested that the difference in the ice nucleation activity of these feldspars is
20 related to the difference in ionic radii of the cations and the local chemical configuration at
21 the surface. They suggested that only potassium feldspar will nucleate ice efficiently because
22 the K^+ is kosmotropic (structure making) in the water hydration shell while Ca^{2+} and Na^+ are
23 chaotropic (structure breaking).

24 There has been much interest in the study of ice nucleation using molecular dynamics
25 simulations (e.g. (Hu and Michaelides, 2007; Cox et al., 2012; Reinhardt and Doye, 2014; Lupi
26 and Molinero, 2014; Lupi et al., 2014; Zielke et al., 2015; Cox et al., 2015a, b; Fitzner et al.,
27 2015). To date there has been little overlap between work of this nature and laboratory
28 experiments. This has been due to difficulties in conducting experiments on similar
29 timescales and spatial extents between real-world and computational systems. While these
30 obstacles are likely to remain in place for some time, the feldspars may offer the opportunity
31 to address this deficit by providing qualitative corroboration between computational and
32 laboratory results. For instance, it may be possible to study ice nucleation on different types
33 of feldspar computationally. If differences in nucleation rate observed also occur in the

1 laboratory greater weight may be placed on mechanisms determined by such studies and so a
2 mechanistic understanding of ice nucleation may be built up.

3 In this paper we have surveyed 15 feldspar samples with varying composition for their ice
4 nucleating ability in the immersion mode. It will be shown that feldspars rich in alkali metal
5 cations tend to be much better at nucleating ice than those rich in calcium. First, we
6 introduce the feldspar group of minerals.

7

8

9 **2 The feldspar group of minerals**

10 The feldspars are tectosilicates (also called framework silicates) with a general formula of
11 $XAl(Si,Al)Si_2O_8$, where X is usually potassium, sodium or calcium (Deer et al., 1992).

12 Unlike clays, which are phyllosilicates (or sheet silicates), tectosilicates are made up of three
13 dimensional frameworks of silica tetrahedra. Substitution of Si with Al in the structure is
14 charge balanced by cation addition or replacement within the cavities in the framework. This
15 leads to a large variability of composition in the feldspars and means that most feldspars in
16 rocks have compositions between end-members of sodium-, calcium- or potassium-feldspars
17 (Deer et al., 1992; Wenk and Bulakh, 2004). A ternary representation of feldspar
18 compositions is shown in Figure 1. All feldspars have very similar crystal structures, but the
19 presence of different ions and degrees of disorder related to the conditions under which they
20 crystallised from the melt (lava or magma) yields subtle differences which can result in
21 differing symmetry.

22 There are three polymorphs (minerals with the same composition, but different crystal
23 structure) of the potassium end-member, which are microcline, orthoclase and sanidine. The
24 polymorphs become more disordered in terms of Al placement in the tetrahedra from
25 microcline to sanidine, respectively. The structures of feldspars which form from a melt vary
26 according to their cooling rate. If cooling is fast (volcanic), sanidine is preserved. If cooling is
27 slow, in some granites for example, microcline may be formed. Feldspars formed in
28 metamorphic rocks have high degrees of Al/Si order. The sodium end-member of the
29 feldspars is albite and the calcium end-member is anorthite. Feldspars with compositions
30 between sodium and calcium form a solid solution and are collectively termed the plagioclase
31 feldspars with specific names for different composition ranges. Feldspars between sodium

1 and potassium end-members are collectively termed the alkali feldspars and can be
2 structurally complex. A solid solution series exists between high albite and sanidine ('high'
3 refers to high temperature character which is preserved on fast cooling), but not between low
4 albite and microcline ('low' refers to low temperature character which is indicative of slow
5 cooling rates). In contrast to the series between sodium and calcium, and sodium and
6 potassium, there are no feldspars between calcium and potassium end-members because
7 calcium and potassium ions do not actively substitute for one another within the framework
8 lattice due their difference in size and ionic charge (Deer et al., 1992;Wenk and Bulakh,
9 2004).

10 There is limited information about the composition of airborne atmospheric mineral dusts
11 (Glaccum and Prospero, 1980;Kandler et al., 2007;Kandler et al., 2009); where mineralogy is
12 reported the breakdown of the feldspar family has only been done in a limited way. Atkinson
13 et al. (2013) compiled the available measurements and grouped them into K-feldspars and
14 plagioclase feldspars (see the Supplementary Table 1 in Atkinson et al. (2013)). This
15 compilation indicates that the feldspar type is highly variable in atmospheric dusts, with K-
16 feldspars ranging from 1 to 25% by mass (with a mean of 5%) and plagioclase feldspars
17 ranging from 1 to 14% (with a mean of 7%). The feldspar component of airborne dusts is
18 highly variable and the nucleating ability of the various components needs to be investigated.

19 In order to aid the discussion and representation of the data we have grouped the feldspars
20 into three groups: the plagioclase feldspars (not including albite), albite (the sodium rich
21 corner of the ternary diagram) and potassium (K-) feldspars (microcline, sanidine and
22 orthoclase). The K-feldspars contain varying amounts of sodium, but their naming is
23 determined by their crystal structure. We also collectively refer to albite and potassium
24 feldspars as alkali feldspars.

25

26 **3 Samples and sample preparation**

27 A total of 15 feldspars were sourced for this study. Details of the plagioclase feldspars tested
28 are in Table 1 and details of the alkali feldspars are in Table 2. We have made use of a series
29 of characterised plagioclase feldspars which were assembled for previous studies (Carpenter
30 et al., 1985;Carpenter, 1986;Carpenter, 1991). The other samples were sourced from a range
31 of repositories, detailed in Tables 1 and 2. The naming convention we have used in this paper

1 is to state the identifier of the specific sample followed by the mineral name. For example,
2 BCS 376 microcline is a microcline sample from the Bureau of Analysed Samples with
3 sample code 376. In other cases, such as Amelia Albite, the sample is from a traceable
4 source and is commonly referred to with this name and when a code is used, such as 97490
5 plagioclase, the code links to the cited publications.

6 Anorthite glass and synthetic anorthite ANC 68 were tested for ice nucleating efficiency to
7 investigate the impact of crystal structure in feldspar. The anorthite glass was produced by
8 Carpenter (1991) by melting natural calcite with reagent grade SiO_2 and Al_2O_3 at 1680°C for
9 3 hours. The melt was then stirred before air cooling. The resulting glass was then annealed at
10 800°C to relieve internal stresses. The composition of the resulting glass was shown to be
11 stoichiometric $\text{CaAl}_2\text{Si}_2\text{O}_8$. Synthetic anorthite ANC 68 was produced by heating a sample of
12 this glass to 1400°C for 170 hours. As these two samples are chemically identical, differing
13 only in that one is amorphous and the other crystalline, comparison of the ice nucleating
14 efficiency of the two samples has the potential to reveal information about the impact of
15 feldspar crystal structure on ice nucleating efficiency. Feldspars 148559, 21704a, 67796b and
16 97490 plagioclase and Amelia albite are natural samples that form a solid solution series
17 covering the plagioclase series from nearly pure anorthite to nearly pure albite as seen in
18 Table 1.

19 The alkali feldspars used here have not previously been characterised. Rietveld refinement of
20 powder XRD patterns was carried out using T O Tal Pattern Analysis Solutions (TOPAS) to
21 determine the phase of the feldspar present. The results of this process are presented in Table
22 2. The surface areas of all the feldspars were measured by Brunauer-Emmett-Teller (BET)
23 nitrogen gas adsorption (see Sect. 4). All samples, unless otherwise stated, were ground to
24 reduce the particle size and increase the specific surface area using a mortar and pestle which
25 were scrubbed with pure quartz then cleaned with deionised water and methanol before use.
26 Grinding of most samples was necessary in order to make the particles small enough for our
27 experiments. Amelia albite was the only material tested both in an unground state (or at least
28 not a freshly ground state) and a freshly ground state. Suspensions of known concentration
29 were made up gravimetrically using Milli-Q water ($18.2 \text{ M}\Omega\cdot\text{cm}$). Except where stated
30 otherwise the suspensions were then mixed for a few minutes using magnetic stirrers prior to
31 use in ice nucleation experiments.

1 The activity of Amelia albite and TUD #3 microcline decrease during repeat experiments
2 conducted approximately 30 minutes after initial experiments. Based on this observation
3 three samples, the BCS 376 microcline, ground Amelia albite and TUD #3 microcline, were
4 tested for changes in ice nucleating efficiency with time, when left in suspension at room
5 temperature. BCS 376 microcline was chosen as it has been previously studied and the
6 activity decrease was not seen on the time scale of ~ 30 minutes previously. Ice nucleation
7 efficiency was quantified at intervals over 11 days. Between experiments the suspensions
8 were left at room temperature without stirring and then stirred to re-suspend the particulates
9 for the ice nucleation experiments. Suspensions of the three dusts were also tested 16 months
10 after initial experiments were performed to determine the long term impact of contact with
11 water on ice nucleation efficiency.

12

13 **4 Experimental method and data analysis**

14 In order to quantify the efficiency with which a range of feldspar dusts nucleate ice we made
15 use of the microliter Nucleation by Immersed Particle Instrument (μ l-NIPI). This system has
16 been used to make numerous ice nucleation measurements in the past and has been described
17 in detail by Whale et al. (2015). Briefly, 1 ± 0.025 μ l droplets of an aqueous suspension,
18 containing a known mass concentration of feldspar particles are pipetted onto a hydrophobic
19 coated glass slide. This slide is placed on a temperature controlled stage and cooled from
20 room temperature at a rate of 5 $^{\circ}\text{C min}^{-1}$ to 0 $^{\circ}\text{C}$ and then at 1 $^{\circ}\text{C min}^{-1}$ until all droplets are
21 frozen. Dry nitrogen is flowed over the droplets at 0.2 l min^{-1} to prevent frozen droplets from
22 affecting neighbouring liquid droplets, droplets evaporate slowly during experiments
23 however this has been shown to have no detectable effect on freezing temperatures (Whale et
24 al., 2015). Whale et al. (2015) demonstrated that a dry nitrogen flow prevents condensation
25 and frost accumulating on the glass slide so ice from a frozen droplet cannot trigger freezing
26 in neighbouring droplets. Freezing is observed with a digital camera, allowing determination
27 of the fraction of droplets frozen as a function of temperature. Multiple experiments have
28 been combined to produce single sets of data for each mineral. Suspensions of the feldspars
29 were made up gravimetrically and specific surface areas of the samples were measured using
30 the Brunauer–Emmett–Teller (BET) N_2 adsorption method using a Micromeritics TriStar
31 3000. Here the μ l-NIPI technique is used to for immersion mode nucleation experiments.

1 To allow comparison of the ability of different materials to nucleate ice, the number of active
2 sites is normalised to the surface area available for nucleation. This yields the ice nucleation
3 active site density, $n_s(T)$. $n_s(T)$ is the number of ice nucleating sites that become active per
4 surface area on cooling from 0°C to temperature T and can be calculated using (Connolly et
5 al., 2009):

$$6 \quad \frac{n(T)}{N} = 1 - \exp(-n_s(T)A) \quad (1)$$

7 Where $n(T)$ is the number of droplets frozen at temperature T , N is the total number of
8 droplets in the experiment and A is the surface area of nucleator per droplet.

9 Active sites may be related to imperfections in a crystal structure, such as cracks or defects,
10 or may be related to the presence of quantities of other more active materials located in
11 specific locations at a surface. While the fundamental nature of active sites is not clear, and
12 may be different for different materials, n_s is a pragmatic parameter which allows us to
13 empirically define the ice nucleating efficiency of a range of materials (Vali, 2014).

14 This description is site specific and does not include time dependence. The role of time
15 dependence in ice nucleation has recently been extensively discussed (Vali, 2014; Vali et al.,
16 2014; Vali, 2008; Herbert et al., 2014; Wright et al., 2013). For feldspar (at least for BCS 376
17 microcline) it is thought that the time dependence of nucleation is relatively weak and that the
18 particle to particle, or active site to active site, variability is much more important (Herbert et
19 al., 2014). The implication of this is that specific sites on the surface of most nucleators,
20 including feldspars, nucleate ice more efficiently than the majority of the surface. As this
21 study is aimed at comparing and assessing the relative ice nucleating abilities of different
22 feldspars we have not determined the time dependence of observed ice nucleation in this
23 work, although this would be an interesting topic for future study.

24 By assuming that the BET surface area of the feldspar powders is made up of monodisperse
25 particles it can be estimated that droplets containing 1 wt% of feldspar will each contain
26 around 10^6 particles. While there will be a distribution of particle sizes we assume that there
27 are enough particles per droplet that the uncertainty in surface area per droplet due to the
28 distribution of particles through the droplets is negligible. In contrast, it has been suggested
29 that ice nucleation data could be explained by variability of nucleator surface area through the
30 droplet population (Alpert and Knopf, 2016). Our assumption that each droplet contains a
31 representative surface area is supported by our previous work where we show that n_s derived

1 from experiments with a range of feldspar concentrations are consistent with one another
 2 (Whale et al., 2015;Atkinson et al., 2013). If the particles were distributed through the
 3 droplets in such a way that some droplet contained a much larger surface area of feldspar than
 4 others we would expect the slope of n_s with temperature to be artificially shallow. The slope
 5 would be artificially shallow because droplets containing more than the average feldspar
 6 surface area would tend to freeze at higher temperatures and vice versa. However, the fact
 7 that n_s data for droplets made from suspensions made up with a wide range of different
 8 feldspar concentrations all line up shows that the droplet to droplet variability in feldspar
 9 surface area is minor (Atkinson et al., 2013;Whale et al., 2015). Hence, the droplet to droplet
 10 variability in feldspar surface area is neglected and the uncertainty in surface area per droplet
 11 in these experiments is estimated from the uncertainties in weighing, pipetting and specific
 12 surface area of the feldspars. Indeed, Murray et al (2011) found that even with picolitre
 13 droplets containing 10's of particles per droplet median nucleation temperatures scaled well
 14 with surface area per droplet calculated in the way used in this work.

15 In order to estimate the uncertainty in $n_s(T)$ due to the randomness of the distribution of the
 16 active sites in droplet freezing experiments, we conducted Monte Carlo simulations. Wright
 17 and Petters (2013) previously adopted a similar approach to simulate the distribution of active
 18 sites in droplet freezing experiments. In these simulations, we generate a list of possible
 19 values for the number of active sites per droplet (μ). The theoretical relationship between the
 20 fraction of droplets frozen and μ can be derived from the Poisson distribution:

$$21 \quad \frac{n(T)}{N} = 1 - \exp(-\mu) \quad (2)$$

22 The simulation works in the following manner. First, we take a value of μ and we simulate a
 23 corresponding random distribution of active sites through the droplet population for an
 24 experiment. Every droplet containing one or more active sites is then considered to be frozen.
 25 In this way, we can obtain a simulated value of the fraction frozen for a certain value of μ .
 26 Repeating this process many times and for all the possible values of μ , we obtain a
 27 distribution of possible values of μ that can explain each value of the observed fraction
 28 frozen. This resulting distribution is neither Gaussian nor symmetric, so in order to propagate
 29 the uncertainty to $n_s(T)$ values, we take the following steps. First, we generate random
 30 values of μ following the corresponding previously simulated distribution for each value of
 31 the fraction frozen. Then, we simulate random values of A following a Gaussian distribution
 32 centred on the value derived from the specific surface area per droplet with the standard

1 deviation derived from the uncertainty in droplet volume and specific surface area. We
2 assume that each droplet contains a representative surface area distribution as discussed
3 above. This process results in two distributions, one for A and one for μ , with these
4 distributions we can calculate the resultant distribution of $n_s(T)$ values, and from that
5 distribution we obtain the 95% confidence interval.

6

7 **5 Results and discussion**

8

9 **5.1 Ice nucleation efficiencies of plagioclase and alkali feldspars**

10 Droplet fraction frozen from μ l-NIPI for the 15 feldspar samples are shown in Figure 2. The
11 values of $n_s(T)$ derived from these experiments are shown in Figure 3 along with the $n_s(T)$
12 parameterisation from Atkinson et al. (2013) for BCS 376 microcline. The various groups of
13 feldspars are indicated by colour which corresponds to the regions of the phase diagram in
14 Figure 1. We define potassium (K-) feldspars (red) as those rich in K including microcline,
15 orthoclase and sanidine; the Na end-member is albite (green); and plagioclase series feldspars
16 (blue) are a solid solution between albite and the calcium end-member, anorthite.

17 Out of the six K-feldspars studied, five fall on or near the line defined by Atkinson et al.
18 (2013). These include three microcline samples and one sanidine sample, which have
19 different crystal structures. Sanidine has disordered Al atoms, microcline has ordered Al
20 atoms and orthoclase has intermediate order; these differences result in differences in
21 symmetry and hence space group (see Tables 1 and 2). The freezing results indicate that Al
22 disordering does not play an important role in nucleation for the analysed weight
23 concentration range. However, one K-feldspar sample, TUD#3 microcline, was substantially
24 more active. This indicates that crystal structure and composition are not the only factors
25 dictating the ice nucleating ability of K-feldspars.

26 All plagioclase feldspars tested were less active ice nucleators than the K-feldspars which
27 were tested. There was relatively little variation in the ice nucleation activities of the
28 plagioclase solid solution series characterised by Carpenter (1986) and Carpenter et al.
29 (1985). For instance, of those feldspars that possess the plagioclase structure, greater sodium
30 content does not systematically increase effectiveness of ice nucleation. Overall, the results

1 for plagioclase feldspars indicate that they have an ice nucleating ability much smaller than
2 that of the K-feldspars.

3 It is also interesting to note that the ANC 68 synthetic anorthite had different nucleating
4 properties to the anorthite glass from which it was crystallised (and had the same
5 composition). The ANC 68 synthetic anorthite sample has a much more shallow $n_s(T)$ curve
6 than the glass. This is noteworthy, because the composition of these two materials is
7 identical, but the phase of the material is different. It demonstrates that crystallinity is not
8 required to cause nucleation, but the presence of crystallinity can provide rare active sites
9 which can trigger nucleation at much higher temperatures. In a future study it would be
10 interesting to attempt to probe the nature of these active sites.

11 We tested three predominantly Na-feldspars (albite). Amelia albite was found to be highly
12 active, approaching that of TUD#3 microcline. The others, BCS 375 albite, and TUD#2 albite
13 were less active, intermediate between the K-feldspars and plagioclase feldspars.

14 To ensure that the high activity of Amelia albite and microcline TUD#3 was not caused by
15 contamination from biological INPs the samples were heated to 100°C in Milli-Q water for
16 15 minutes. This treatment will disrupt any protein based nucleators present (O'Sullivan et
17 al., 2015). No significant reduction in freezing temperatures (beyond what would be expected
18 from the activity decay described in Sect. 5.2) was observed suggesting that the highly active
19 INPs present are associated with the feldspars rather than biological protein contamination.
20 Certain biological nucleators have been observed to retain their ice nucleating activity despite
21 heat treatment of this type (Pummer et al., 2012; O'Sullivan et al., 2014; Tobo et al., 2014)
22 however, to the best of our knowledge, no biological species has been observed to nucleate
23 ice at such warm temperatures after heat treatment. This behaviour does not seem consistent
24 with biological nucleators, unless the biological entity is within the Amelia albite particles
25 and is somehow dispersed through the particle population during grinding. While we cannot
26 exclude the possibility that some unknown biological species is present on microcline TUD#3
27 and Amelia albite it seems more likely that the minerals themselves are responsible for the
28 observed ice nucleation activity. Additionally, it is known that certain organic molecules can
29 nucleate ice efficiently (Fukuta, 1966). It is not possible to exclude the possibility of the
30 presence of these or other, unknown, heat resistant contaminants that nucleate ice very
31 efficiently.

1 It has been noted by Vali (2014) that there is an indication that nucleators which are more
2 active at higher temperatures tend to have steeper slopes of $\ln J$ (nucleation rate). We have
3 observed this trend here in the data shown in Figure 3 ($n_s(T)$ is proportional to J for a single
4 component). The slopes of experiments where freezing occurred at lower temperatures
5 (plagioclases) generally being flatter than those where freezing took place at higher
6 temperatures (alkali feldspars). Vali (2014) suggests that this maybe the result of different
7 observational methods. In this study we have used a single method for all experiments so the
8 trend is unlikely to be due to an instrument artefact. The implication is that active sites with
9 lower activity tend to be more diverse in nature. This may indicate that there are fewer
10 possible ways to compose an active site that is efficient at nucleating ice and that there will
11 be less variation in these sites as a result. The active sites of lower activity may take a greater
12 range of forms and so encompass a greater diversity of freezing temperatures. The lower
13 diversity in the sites active at higher temperatures may explain the steep slopes in n_s seen,
14 however it should be noted that classical nucleation theory also predicts steeper slopes at
15 higher temperatures assuming a single contact angle.

16 To summarise, plagioclase feldspars tend to have relatively poor ice nucleating abilities, all
17 K-feldspars we tested are relatively good at nucleating ice and the albites are variable in their
18 nucleating activity. Out of the six K-feldspars tested, five have very similar activities and are
19 well approximated by the parameterisation of Atkinson et al. (2013) in the temperature- n_s
20 regime we investigated here. However, we have identified two alkali feldspar samples, one
21 K-feldspar and one albite, which are much more active than the others indicating that a factor
22 or factors other than the polymorph or composition determines the efficiency of alkali
23 feldspars as ice nucleators.

24 **5.2 The stability of active sites**

25 It was observed that the ice nucleation activity of ground Amelia albite and ground TUD #3
26 microcline declined over the course of ~30 minutes. Only the initial run is shown in Figure 3
27 where the feldspar had spent only about 10 minutes in suspension. This decay in activity over
28 the course of ~30 mins was not seen in the other feldspars. To investigate this effect samples
29 of BCS 376 microcline, Amelia albite and TUD #3 microcline were left in water within a
30 sealed vial and tested at intervals over the course of 16 months, with a focus on the first 11
31 days. TUD #3 microcline and Amelia albite were chosen for this experiment as they
32 contained highly active sites, represented two different types of feldspar and were the only

1 feldspars observed to exhibit this rapid decay in activity. BCS 376 microcline was also
2 included in this activity decay experiment as it had provided consistent data over repeated
3 runs and served as a standard in the Atkinson et al. (2013) paper which could therefore be
4 tested. The results of these experiments are shown in Figure 4. The median freezing
5 temperature of the Amelia albite sample was most sensitive to time spent in water, decreasing
6 by 8 °C in 11 days and by 16 °C in 16 months. The TUD#3 microcline sample decreased by
7 about 2 °C in 16 months, but the freezing temperatures of the BCS 376 did not change
8 significantly over 16 months (within the temperature uncertainty of $\pm 0.4^\circ\text{C}$). Clearly, the
9 stability of the active sites responsible for ice nucleation in these samples is highly variable.

10 Amelia albite is a particularly interesting case, where the highly active sites are also highly
11 unstable. For Amelia albite we observed that the ice nucleation ability of the powder directly
12 as supplied (the sample had been ground many years prior to experiments) was much lower
13 than the freshly ground sample. The n_s values for the ‘as-supplied’ Amelia albite are shown in
14 Figure 4. This suggests that the active sites on Amelia albite are unstable and in general are
15 sensitive to the history of the sample. We note that from previous work that BCS 376 feldspar
16 ground to varied extents nucleates ice similarly (Whale et al., 2015) and we have not
17 observed a decay of active sites of the BCS 376 microcline sample when stored in a dry vial
18 over the course of two years. It is also worth noting that freshly ground BCS 376 microcline
19 did not nucleate ice as efficiently as Amelia albite or TUD#3 microcline. These results
20 indicate that BCS 376 microcline contains very active sites, but that these sites are much
21 more stable than those found in Amelia albite. This result is in agreement with the
22 observation that albite weathers faster than microcline in soils as Na^+ is more readily
23 substituted for hydrogen than K^+ (Busenberg and Clemency, 1976; Blum, 1994).

24 Zolles et al. (2015) have suggested that grinding can lead to active sites being revealed, or the
25 enhancement of existing active sites. It was shown in Whale et al. (2015) that differently
26 ground samples of BCS 376 microcline nucleate ice similarly. In contrast Hiranuma et al.
27 (2014) show that ground hematite nucleates ice more efficiently (normalised to surface area)
28 than cubic hematite. The evidence suggests that the ice nucleating efficiencies of different
29 materials respond differently to grinding processes. Indeed, it is evident from this study that
30 highly active sites in Amelia albite are generated by grinding but lose activity when exposed
31 to liquid water, and probably lose activity during exposure to (presumably wet) air, returning
32 to an activity level comparable to that of the plagioclase feldspars. TUD#3 microcline also
33 possesses a highly active site type sensitive to water exposure but falls back to a level of

1 activity higher than the other K-feldspars we have tested. This second, less active site type is
2 shown to be stable in water over the course of 16 months. TUD#3 must possess populations
3 of both more active, unstable sites and less active (although still relatively active compared to
4 the sites on other K-feldspars) stable sites. Amelia albite possesses only unstable sites and
5 much less active sites similar to those found on the plagioclase feldspars we have tested.

6 These results indicate something of the nature of the active sites on feldspars. Throughout
7 this paper we refer to nucleation occurring on active sites, or specific sites, on the surface of
8 feldspar. It is thought that nucleation by most ice active minerals is consistent with nucleation
9 on active sites with a broad spectrum of activities (Marcolli et al., 2007; Lüönd et al.,
10 2010; Niedermeier et al., 2010; Augustin-Bauditz et al., 2014; Herbert et al., 2014; Vali,
11 2014; Wex et al., 2014; Wheeler et al., 2015; Hiranuma et al., 2015; Niedermeier et al.,
12 2015; Hartmann et al., 2016). However, the nature of these active sites is not known. It is
13 postulated that active sites are related to defects in the structure and therefore that each site
14 has a characteristic nucleation ability, producing a spectrum of active sites. Defects are
15 inherently less stable than the bulk of the crystal and we might expect these sites to be
16 affected by dissolution processes, or otherwise altered, in preference to the bulk of the crystal
17 (Parsons et al., 2015). The fact that we observe ice nucleation by populations of active sites
18 with different stabilities in water implies that these sites have different physical or chemical
19 characteristics. Furthermore, the fact that some populations of active sites are sensitive to
20 exposure to water suggests that the history of particles can be critical in determining the ice
21 nucleating ability of mineral dusts. This raises the question of whether differences in ice
22 nucleation efficiency observed by different instruments (Emersic et al., 2015; Hiranuma et al.,
23 2015), could be related to the different conditions particles experience prior to nucleation.

24 **5.3 Comparison to literature data**

25 We have compared the $n_s(T)$ values for various feldspars from a range of literature sources
26 with data from this study in Figure 5. Inspection of this plot confirms that K-feldspars
27 nucleate ice more efficiently than the plagioclase feldspars. Also, with the exception of the
28 hyper-active Amelia albite sample, the K-feldspars are more active than the albites.

29 Results for BCS 376 microcline have been reported in several papers (Atkinson et al.,
30 2013; O'Sullivan et al., 2014; Whale et al., 2015; Emersic et al., 2015). There is a discrepancy
31 between the cloud chamber data from Emersic et al. (2015) and the picolitre droplet cold
32 stage experiments at around -18°C , whereas the data at about -25°C are in agreement.

1 Emersic et al. (2015) attribute this discrepancy to aggregation of feldspar particles in
2 microlitre scale droplet freezing experiments reducing the surface area of feldspar exposed to
3 water leading to a lower $n_s(T)$ value. It is unlikely that this effect can account for the
4 discrepancy because in the temperature range of the Emersic et al. (2015) data the
5 comparison is being made to results from picolitre droplet freezing experiments which
6 Emersic et al. (2015) argue should not be affected by aggregation because there are not
7 enough particles present in each droplet to result in significant aggregation. Atkinson et al.
8 (2013) estimated that on average even the largest droplets only contained a few 10s of
9 particles. We also note that our microscope images of droplets show many individual
10 particles moving independently around in the picolitre droplets in those experiments,
11 indicating that the feldspar grains do not aggregate substantially. Hence, the discrepancy
12 between the data of Emersic et al. (2015) and Atkinson et al. (2013) at around -18°C cannot
13 be accounted for by aggregation. Furthermore, Atkinson et al. (2013) report that the surface
14 area determined from the laser diffraction size distribution of BCS 376 microcline in
15 suspension is 3.5 times smaller than that derived by the gas adsorption measurements (see
16 supplementary Figure 5 in Atkinson et al. (2013) and the corresponding discussion). This
17 difference in surface area can be accounted for by the fact that feldspar grains are not smooth
18 spheres, as assumed in the analysis of the laser diffraction data. Feldspar grains are well-
19 known to be rough and aspherical (Hodson et al., 1997). Atkinson et al. (2013) also note that
20 the laser diffraction technique lacks sensitivity to the smallest particles in the distribution
21 which will also lead to an underestimate in surface area. Nevertheless, the data presented by
22 Atkinson et al. (2013) suggests that aggregation of feldspar particles leading to reduced
23 surface area is at most a minor effect. As such the discrepancy between different instruments
24 remains unexplained and more work is needed on this topic.

25 Ice nucleation by single size-selected particles of TUD#1 microcline has been investigated by
26 Niedermeier et al. (2015) at temperatures below -23°C . We found that TUD#1 microcline
27 was in good agreement with the K-feldspar parameterisation from Atkinson et al. (2013)
28 between about -6 and -11°C . Between -23 and -25°C , the $n_s(T)$ values produced by
29 Niedermeier et al. (2015) are similar (lower by a factor of roughly 4) to that of the Atkinson
30 et al. (2013) parameterisation, despite the different sample types. Niedermeier et al. (2015)
31 used the Leipzig Aerosol Cloud Interaction Simulator (LACIS), in which they size selected
32 particles, activated them to cloud droplets and then quantified the probability of freezing at a
33 particular temperature. It is interesting that the Niedermeier et al. (2015) $n_s(T)$ values curve

1 off at lower temperatures to a limiting value which they term n_s^* , indicating that nucleation
2 by K-feldspars may hit a maximum value and emphasises why we need to be cautious in
3 extrapolating $n_s(T)$ parameterisations beyond the range of experimental data.

4 The data for a microcline, a plagioclase (andesine) and albite from Zolles et al. (2015) is
5 consistent with our finding that plagioclase feldspars are less effective nucleators than K-
6 feldspars. It is also consistent with Atkinson et al. (2013) who found that albite is less
7 efficient at nucleating ice than microcline. However, the data for K-feldspar from Zolles et al.
8 (2015) sits below the line from Atkinson et al. (2013) for BCS 376 microcline and are lower
9 than the points from Niedermeier et al. (2015) for TUD#1 microcline. Their measurements
10 involved making up suspensions (2-5wt%) and then creating a water-in-oil emulsion where
11 droplets were between 10-40 μm . They quote their particle sizes as being between 1-10 μm
12 for the feldspars. Atkinson et al. (2013) worked with 0.8 wt% suspensions, with droplets of 9
13 to 19 μm where the mode particle size was ~ 700 nm. Hence, Zolles et al. (2015) worked with
14 more concentrated suspensions and larger particles than used by Atkinson et al. (2013). In
15 principle, n_s should be independent of droplet volume and particle concentration, but
16 differences between instruments and methods have been reported (Hiranuma et al., 2015).
17 Additionally, Zolles et al. (2015) estimated the surface area of their feldspar particles using a
18 combination of SEM images and the BET surface area of quartz. This leads to an unspecified
19 uncertainty in their n_s values. However, it is not possible to determine whether the observed
20 difference in n_s is due to differences in the sample or the techniques used, but may mean that
21 certain K-feldspars nucleate ice less well than those defined by the Atkinson et al. (2013) line
22 in this temperature regime. This would be a very interesting result as it may provide a point
23 of difference that could provide insight into why K-feldspars nucleate ice efficiently. There
24 has been relatively little work on what makes feldspar a good nucleator of ice. Zolles et al.
25 (2015) suggest that only K-feldspars will nucleate ice well on the basis that Ca^{2+} and Na^+ are
26 chaotropic (structure breaking in water) while K^+ is kosmotropic (structure making in water).
27 We have only observed one feldspar that contains little K^+ but nucleates ice relatively
28 efficiently, Amelia albite. This feldspar loses its activity quickly in water and eventually
29 becomes more comparable to the plagioclase feldspars. It may be that the strong nucleation
30 observed is associated with the small amount of K^+ it contains and that once this dissolves
31 away the feldspar behaves like a plagioclase.

32 Augustin-Bauditz et al. (2014) tentatively concluded that microcline may nucleate ice more
33 efficiently than orthoclase at $n_s(T)$ values above about 10^6 cm^{-2} and at temperatures below -

1 23°C, the conditions where they performed their measurements. They arrived at this
2 conclusion by noting that NX-illite and Arizona test dust both contain orthoclase (8 and 20%,
3 respectively), but the $n_s(T)$ values they report for these materials are more than one order less
4 than microcline.

5 Within the surface area regime examined in this study we have observed some variability
6 amongst the K-feldspars (see Figure 2), but no difference between sanidine and four out of
7 five microclines which fall around the line defined by Atkinson et al. (2013). As discussed
8 above, the Al in sanidine is the least ordered, with microcline the most ordered and orthoclase
9 at an intermediate order, hence we observe no clear dependency on the ordering of Al in K-
10 feldspars. Further investigations of the ice nucleating ability of the various K-feldspar phases
11 at low temperature would be valuable. We could not do this in the present study with the
12 samples used here because we did not have sufficient quantities of the samples.

13

14 **6 Conclusions**

15 In this study we have analysed the ice nucleating ability of 15 characterised feldspar samples.
16 These minerals include plagioclase feldspars (in the solid solution series between Ca and Na
17 end-members), the K-feldspars (sanidine and microcline) and albite (the Na end-member).
18 The results indicate that the alkali feldspars, including albite and K-feldspars, tend to nucleate
19 ice more efficiently than plagioclase feldspars. The plagioclase feldspars nucleate ice at the
20 lowest temperatures with no obvious dependence on the Ca-Na ratio. The albites have a wide
21 variety of nucleating abilities, with one sample nucleating ice much more efficiently than the
22 microcline sample Atkinson et al. (2013) studied. This hyper-active albite lost its activity
23 over time while suspended in water. Five out of six of the K-feldspar samples we studied
24 nucleated ice with a similar efficiency to the BCS 376 microcline studied by Atkinson et al.
25 (2013). A single K-feldspar we studied had a very high activity, nucleating ice as warm as -
26 2°C in our microliter droplet assay. The striking activity of this hyperactive microcline
27 decayed with time spent in water, but not to the same extent as the hyperactive albite sample.
28 While the hyperactive sites are sensitive, to varying degrees, to time spent in water, the
29 activity of the BCS 376 microcline sample used by Atkinson et al. (Atkinson et al., 2013) did
30 not change significantly. We have not excluded the possibility that other entities on the
31 surfaces of the feldspar may be responsible for the ice nucleation observed.

1 In light of these findings, we suggest that there are at least three classes of active site present
2 in the feldspars studied here: *i*) sites of relatively low activity associated with plagioclase
3 feldspars; *ii*) sites which are more active associated with K-feldspars that are stable in water
4 over the course of many months; *iii*) hyper-active sites associated with one albite and one K-
5 feldspar that we studied that loses activity when exposed to water. It is possible that the sites
6 of type *i* are present on the typical K-feldspars, but we do not observe them because ice
7 nucleates on more active sites. Whether these different sites are all related to similar features
8 on the surfaces or if they are each related to different types of features is not known.
9 Nevertheless, it appears that feldspars are characterised by a range of active site types with
10 varying stability and activity.

11 The specific details of these active sites continue to elude us, although it appears that they are
12 only present in alkali feldspars and in particular, the K-feldspars. Unlike the plagioclase
13 feldspars which form a solid solution, the Na and K feldspars in alkali feldspars are often
14 exsolved, possessing intergrowths of the Na and K feldspars referred to as microtexture
15 (Parsons et al., 2015). It is possible that the boundaries between the two phases in the
16 intergrowth provide sites for nucleation that are not present in plagioclase feldspars. If the
17 high energy defects along exsolution boundaries are responsible for higher ice nucleation
18 activity of K-feldspars then this may offer an insight into acid passivation of ice nucleating
19 ability observed in laboratory studies (Wex et al., 2014; Augustin-Bauditz et al., 2014).
20 Berner and Holdren (1979) suggest that the acid mediated weathering of feldspar occurs in
21 multiple stages and suggest dissolution of feldspars is concentrated at high surface energy
22 sites such as dislocations and crystal defects, sites which may be related to ice nucleation.
23 More work is needed to explore the significance of exsolution, microtexture and the impact
24 of weathering on feldspars with respect to ice nucleation activity.

25 In a previous study Atkinson et al. (2013) used an $n_s(T)$ parameterisation of a single K-
26 feldspar (BCS 376 microcline) to approximate the ice nucleating properties of desert dust in a
27 global aerosol model. Given that five out of six of the K-feldspars we studied here have very
28 similar ice nucleating abilities, this approximation seems reasonable. However, we have
29 identified two hyper-active feldspars and do not know how representative these samples are
30 of natural feldspars in dust emission regions. We also note that the active sites on these
31 feldspars are less stable than those of BCS 376 microcline. Nevertheless, there is the
32 possibility that the parameterisation used by Atkinson et al. (2013) underestimates the
33 contribution of feldspars at higher temperatures above about -15°C .

1 In the longer term it may be possible to identify what it is that leads to the variation in ice
2 nucleation activity between the different feldspar classes. In particular, the nature of the
3 active sites in the hyper-active feldspars and the reason plagioclase is so much poorer at
4 nucleating ice are subjects of interest. The instability of the active sites in the hyperactive
5 feldspars may be related to dissolution of feldspar in water and investigation of this process
6 may allow progress towards understanding of nucleation by feldspars. The results presented
7 here are empirical in nature and do not provide a thorough underpinning understanding of the
8 nature of the active sites. Nevertheless, the fact that the feldspar group of minerals have
9 vastly different ice nucleating properties despite possessing very similar crystal structures
10 may provide us with a means of gaining a fundamental insight to heterogeneous ice
11 nucleation.

12

13

14 **Acknowledgments**

15 We would like to acknowledge Theodore Wilson and Alexei Kiselev for helpful discussions
16 and John Morris for introducing TFW and MAC. We are grateful to Alexei Kiselev and
17 Martin Ebert for providing the TUD samples. Alex Harrison thanks the School of Earth and
18 Environment for an Undergraduate Research Scholarship which allowed him to make many
19 of the measurements presented in this paper. We would like to thank the National
20 Environmental Research Council, (NERC, NE/I013466/1; NE/I020059/1; NE/K004417/1;
21 NE/I019057/1; NE/M010473/1) the European Research Council (ERC, 240449 ICE; 632272
22 IceControl; 648661 MarineIce), and the Engineering and Physical Sciences Research Council
23 (EPSRC, EP/M003027/1) for funding.

24

25

26 Alpert, P. A., and Knopf, D. A.: Analysis of isothermal and cooling-rate-dependent immersion freezing
27 by a unifying stochastic ice nucleation model, *Atmos. Chem. Phys.*, 16, 2083-2107, 10.5194/acp-16-
28 2083-2016, 2016.

29

30 Atkinson, J. D., Murray, B. J., Woodhouse, M. T., Whale, T. F., Baustian, K. J., Carslaw, K. S., Dobbie,
31 S., O'Sullivan, D., and Malkin, T. L.: The importance of feldspar for ice nucleation by mineral dust in
32 mixed-phase clouds, *Nature*, 498, 355-358, 10.1038/nature12278, 2013.

33

- 1 Augustin-Bauditz, S., Wex, H., Kanter, S., Ebert, M., Niedermeier, D., Stolz, F., Prager, A., and
2 Stratmann, F.: The immersion mode ice nucleation behavior of mineral dusts: A comparison of
3 different pure and surface modified dusts, *Geophys. Res. Lett.*, 41, 7375-7382,
4 10.1002/2014gl061317, 2014.
5
- 6 Berner, R. A., and Holdren, G. R.: Mechanism of feldspar weathering—ii. Observations of feldspars
7 from soils, *Geochim. Cosmochim. Acta*, 43, 1173-1186, [http://dx.doi.org/10.1016-](http://dx.doi.org/10.1016/0016-7037(79)90110-8)
8 [7037\(79\)90110-8](http://dx.doi.org/10.1016/0016-7037(79)90110-8), 1979.
9
- 10 Blum, A. E.: Feldspars in weathering, in: *Feldspars and their reactions*, Springer, 595-630, 1994.
11
- 12 Busenberg, E., and Clemency, C. V.: The dissolution kinetics of feldspars at 25 c and 1 atm co2 partial
13 pressure, *Geochim. Cosmochim. Acta*, 40, 41-49, 1976.
14
- 15 Carpenter, M.: Experimental delineation of the “e” \rightleftharpoons i\bar 1 and “e” \rightleftharpoons c\bar 1 transformations in
16 intermediate plagioclase feldspars, *Phys Chem Minerals*, 13, 119-139, 10.1007/bf00311902, 1986.
17
- 18 Carpenter, M. A., McConnell, J. D. C., and Navrotsky, A.: Enthalpies of ordering in the plagioclase
19 feldspar solid solution, *Geochim. Cosmochim. Acta*, 49, 947-966, [http://dx.doi.org/10.1016/0016-](http://dx.doi.org/10.1016/0016-7037(85)90310-2)
20 [7037\(85\)90310-2](http://dx.doi.org/10.1016/0016-7037(85)90310-2), 1985.
21
- 22 Carpenter, M. A.: Mechanisms and kinetics of al-si ordering in anorthite; i, incommensurate
23 structure and domain coarsening, *American Mineralogist*, 76, 1110-1119, 1991.
24
- 25 Connolly, P. J., Möhler, O., Field, P. R., Saathoff, H., Burgess, R., Chouarton, T., and Gallagher, M.:
26 Studies of heterogeneous freezing by three different desert dust samples, *Atmos. Chem. Phys.*, 9,
27 2805-2824, 10.5194/acp-9-2805-2009, 2009.
28
- 29 Cox, S. J., Kathmann, S. M., Purton, J. A., Gillan, M. J., and Michaelides, A.: Non-hexagonal ice at
30 hexagonal surfaces: The role of lattice mismatch, *Phys. Chem. Chem. Phys.*, 14, 7944-7949,
31 10.1039/c2cp23438f, 2012.
32
- 33 Cox, S. J., Kathmann, S. M., Slater, B., and Michaelides, A.: Molecular simulations of heterogeneous
34 ice nucleation. I. Controlling ice nucleation through surface hydrophilicity, *The Journal of Chemical*
35 *Physics*, 142, 184704, doi:<http://dx.doi.org/10.1063/1.4919714>, 2015a.
36
- 37 Cox, S. J., Kathmann, S. M., Slater, B., and Michaelides, A.: Molecular simulations of heterogeneous
38 ice nucleation. II. Peeling back the layers, *The Journal of Chemical Physics*, 142, 184705,
39 doi:<http://dx.doi.org/10.1063/1.4919715>, 2015b.
40
- 41 Deer, W. A., Howie, R. A., and Zussman, J.: *An introduction to the rock forming minerals*, 2nd ed.,
42 Addison Wesley Longman, Harlow, UK, 1992.
43

- 1 DeMott, P. J., Sassen, K., Poellot, M. R., Baumgardner, D., Rogers, D. C., Brooks, S. D., Prenni, A. J.,
2 and Kreidenweis, S. M.: African dust aerosols as atmospheric ice nuclei, *Geophys. Res. Lett.*, 30,
3 1732, 10.1029/2003GL017410, 2003.
4
- 5 Emersic, C., Connolly, P. J., Boulton, S., Campana, M., and Li, Z.: Investigating the discrepancy between
6 wet-suspension- and dry-dispersion-derived ice nucleation efficiency of mineral particles, *Atmos.*
7 *Chem. Phys.*, 15, 11311-11326, 10.5194/acp-15-11311-2015, 2015.
8
- 9 Fitzner, M., Sosso, G. C., Cox, S. J., and Michaelides, A.: The many faces of heterogeneous ice
10 nucleation: Interplay between surface morphology and hydrophobicity, *J. Am. Chem. Soc.*, 137,
11 13658-13669, 10.1021/jacs.5b08748, 2015.
12
- 13 Freedman, M. A.: Potential sites for ice nucleation on aluminosilicate clay minerals and related
14 materials, *The Journal of Physical Chemistry Letters*, 2015.
15
- 16 Fukuta, N.: Experimental studies of organic ice nuclei, *J. Atmos. Sci.*, 23, 191-196, doi:10.1175/1520-
17 0469(1966)023<0191:ESOOIN>2.0.CO;2, 1966.
18
- 19 Ginoux, P., Prospero, J. M., Gill, T. E., Hsu, N. C., and Zhao, M.: Global-scale attribution of
20 anthropogenic and natural dust sources and their emission rates based on modis deep blue aerosol
21 products, *Rev. Geophys.*, 50, RG3005, 10.1029/2012rg000388, 2012.
22
- 23 Glaccum, R. A., and Prospero, J. M.: Saharan aerosols over the tropical north-atlantic - mineralogy,
24 *Mar. Geol.*, 37, 295-321, 10.1016/0025-3227(80)90107-3, 1980.
25
- 26 Hartmann, S., Wex, H., Clauss, T., Augustin-Bauditz, S., Niedermeier, D., Rösch, M., and Stratmann,
27 F.: Immersion freezing of kaolinite: Scaling with particle surface area, *J. Atmos. Sci.*, 73, 263-278,
28 doi:10.1175/JAS-D-15-0057.1, 2016.
29
- 30 Herbert, R. J., Murray, B. J., Whale, T. F., Dobbie, S. J., and Atkinson, J. D.: Representing time-
31 dependent freezing behaviour in immersion mode ice nucleation, *Atmos. Chem. Phys.*, 14, 8501-
32 8520, 10.5194/acp-14-8501-2014, 2014.
33
- 34 Herbert, R. J., Murray, B. J., Dobbie, S. J., and Koop, T.: Sensitivity of liquid clouds to homogenous
35 freezing parameterizations, *Geophys. Res. Lett.*, 42, 1599-1605, 10.1002/2014gl062729, 2015.
36
- 37 Hiranuma, N., Hoffmann, N., Kiselev, A., Dreyer, A., Zhang, K., Kulkarni, G., Koop, T., and Möhler, O.:
38 Influence of surface morphology on the immersion mode ice nucleation efficiency of hematite
39 particles, *Atmos. Chem. Phys.*, 14, 2315-2324, 10.5194/acp-14-2315-2014, 2014.
40
- 41 Hiranuma, N., Augustin-Bauditz, S., Bingemer, H., Budke, C., Curtius, J., Danielczok, A., Diehl, K.,
42 Dreischmeier, K., Ebert, M., Frank, F., Hoffmann, N., Kandler, K., Kiselev, A., Koop, T., Leisner, T.,
43 Möhler, O., Nillius, B., Peckhaus, A., Rose, D., Weinbruch, S., Wex, H., Boose, Y., DeMott, P. J., Hader,

1 J. D., Hill, T. C. J., Kanji, Z. A., Kulkarni, G., Levin, E. J. T., McCluskey, C. S., Murakami, M., Murray, B. J.,
2 Niedermeier, D., Petters, M. D., O'Sullivan, D., Saito, A., Schill, G. P., Tajiri, T., Tolbert, M. A., Welti,
3 A., Whale, T. F., Wright, T. P., and Yamashita, K.: A comprehensive laboratory study on the
4 immersion freezing behavior of illite nx particles: A comparison of 17 ice nucleation measurement
5 techniques, *Atmos. Chem. Phys.*, 15, 2489-2518, 10.5194/acp-15-2489-2015, 2015.
6

7 Hodson, M. E., Lee, M. R., and Parsons, I.: Origins of the surface roughness of unweathered alkali
8 feldspar grains, *Geochim. Cosmochim. Acta*, 61, 3885-3896, 10.1016/s0016-7037(97)00197-x, 1997.
9

10 Hoose, C., Lohmann, U., Erdin, R., and Tegen, I.: The global influence of dust mineralogical
11 composition on heterogeneous ice nucleation in mixed-phase clouds, *Environ. Res. Lett.*, 3,
12 10.1088/1748-9326/3/2/025003, 2008.
13

14 Hoose, C., Kristjánsson, J. E., Chen, J.-P., and Hazra, A.: A classical-theory-based parameterization of
15 heterogeneous ice nucleation by mineral dust, soot, and biological particles in a global climate
16 model, *J. Atmos. Sci.*, 67, 2483-2503, 10.1175/2010jas3425.1, 2010.
17

18 Hoose, C., and Möhler, O.: Heterogeneous ice nucleation on atmospheric aerosols: A review of
19 results from laboratory experiments, *Atmos. Chem. Phys.*, 12, 9817-9854, 10.5194/acp-12-9817-
20 2012, 2012.
21

22 Hu, X. L., and Michaelides, A.: Ice formation on kaolinite: Lattice match or amphoterism?, *Surface*
23 *Science*, 601, 5378-5381, 10.1016/j.susc.2007.09.012, 2007.
24

25 Kandler, K., Benker, N., Bundke, U., Cuevas, E., Ebert, M., Knippertz, P., Rodríguez, S., Schütz, L., and
26 Weinbruch, S.: Chemical composition and complex refractive index of saharan mineral dust at izana,
27 tenerife (spain) derived by electron microscopy, *Atmos. Environ.*, 41, 8058-8074, 2007.
28

29 Kandler, K., Schütz, L., Deutscher, C., Ebert, M., Hofmann, H., Jäckel, S., Jaenicke, R., Knippertz, P.,
30 Lieke, K., Massling, A., Petzold, A., Schladitz, A., Weinzierl, B., Wiedensohler, A., Zorn, S., and
31 Weinbruch, S.: Size distribution, mass concentration, chemical and mineralogical composition and
32 derived optical parameters of the boundary layer aerosol at tinfou, morocco, during samum 2006,
33 *Tellus*, 61B, 32-50, 10.1111/j.1600-0889.2008.00385.x, 2009.
34

35 Kandler, K., SchÜTz, L., JÄCkel, S., Lieke, K., Emmel, C., MÜLLer-Ebert, D., Ebert, M., Scheuvs, D.,
36 Schladitz, A., ŠEgviĆ, B., Wiedensohler, A., and Weinbruch, S.: Ground-based off-line aerosol
37 measurements at praia, cape verde, during the saharan mineral dust experiment: Microphysical
38 properties and mineralogy, *Tellus*, 63B, 459-474, 10.1111/j.1600-0889.2011.00546.x, 2011.
39

40 Lüönd, F., Stetzer, O., Welti, A., and Lohmann, U.: Experimental study on the ice nucleation ability of
41 size-selected kaolinite particles in the immersion mode, *J. Geophys. Res.*, 115, D14201,
42 10.1029/2009jd012959, 2010.
43

1 Lupi, L., Hudait, A., and Molinero, V.: Heterogeneous nucleation of ice on carbon surfaces, *J. Am.*
2 *Chem. Soc.*, 136, 3156-3164, 10.1021/ja411507a, 2014.
3

4 Lupi, L., and Molinero, V.: Does hydrophilicity of carbon particles improve their ice nucleation
5 ability?, *J. Phys. Chem. A*, 118, 7330-7337, 10.1021/jp4118375, 2014.
6

7 Marcolli, C., Gedamke, S., Peter, T., and Zobrist, B.: Efficiency of immersion mode ice nucleation on
8 surrogates of mineral dust, *Atmos. Chem. Phys.*, 7, 5081-5091, 10.5194/acp-7-5081-2007, 2007.
9

10 Murray, B. J., Broadley, S. L., Wilson, T. W., Atkinson, J. D., and Wills, R. H.: Heterogeneous freezing
11 of water droplets containing kaolinite particles, *Atmos. Chem. Phys.*, 11, 4191-4207, 10.5194/acp-
12 11-4191-2011, 2011.
13

14 Murray, B. J., O'Sullivan, D., Atkinson, J. D., and Webb, M. E.: Ice nucleation by particles immersed in
15 supercooled cloud droplets, *Chem. Soc. Rev.*, 41, 6519-6554, 10.1039/C2CS35200A, 2012.
16

17 Niedermeier, D., Hartmann, S., Shaw, R. A., Covert, D., Mentel, T. F., Schneider, J., Poulain, L., Reitz,
18 P., Spindler, C., Clauss, T., Kiselev, A., Hallbauer, E., Wex, H., Mildenerger, K., and Stratmann, F.:
19 Heterogeneous freezing of droplets with immersed mineral dust particles - measurements and
20 parameterization, *Atmos. Chem. Phys.*, 10, 3601-3614, 10.5194/acp-10-3601-2010, 2010.
21

22 Niedermeier, D., Augustin-Bauditz, S., Hartmann, S., Wex, H., Ignatius, K., and Stratmann, F.: Can we
23 define an asymptotic value for the ice active surface site density for heterogeneous ice nucleation?,
24 *Journal of Geophysical Research: Atmospheres*, 120, 5036-5046, 10.1002/2014jd022814, 2015.
25

26 Niemand, M., Möhler, O., Vogel, B., Vogel, H., Hoose, C., Connolly, P., Klein, H., Bingemer, H.,
27 DeMott, P. J., Skrotzki, J., and Leisner, T.: A particle-surface-area-based parameterization of
28 immersion freezing on desert dust particles, *J. Atmos. Sci.*, 69, 10.1175/jas-d-11-0249.1, 2012.
29

30 O'Sullivan, D., Murray, B. J., Malkin, T. L., Whale, T. F., Umo, N. S., Atkinson, J. D., Price, H. C.,
31 Baustian, K. J., Browse, J., and Webb, M. E.: Ice nucleation by fertile soil dusts: Relative importance
32 of mineral and biogenic components, *Atmos. Chem. Phys.*, 14, 1853-1867, 10.5194/acp-14-1853-
33 2014, 2014.
34

35 O' Sullivan, D., Murray, B. J., Ross, J. F., Whale, T. F., Price, H. C., Atkinson, J. D., Umo, N. S., and
36 Webb, M. E.: The relevance of nanoscale biological fragments for ice nucleation in clouds, *Sci. Rep.*,
37 5, 10.1038/srep08082, 2015.
38

39 Parsons, I., Fitz Gerald, J. D., and Lee, M. R.: Routine characterization and interpretation of complex
40 alkali feldspar intergrowths, *American Mineralogist*, 100, 1277-1303, 10.2138/am-2015-5094, 2015.
41

1 Perlwitz, J. P., Pérez García-Pando, C., and Miller, R. L.: Predicting the mineral composition of dust
2 aerosols – part 1: Representing key processes, *Atmos. Chem. Phys.*, 15, 11593-11627, 10.5194/acp-
3 15-11593-2015, 2015.
4

5 Pummer, B. G., Bauer, H., Bernardi, J., Bleicher, S., and Grothe, H.: Suspendable macromolecules are
6 responsible for ice nucleation activity of birch and conifer pollen, *Atmos. Chem. Phys.*, 12, 2541-
7 2550, 10.5194/acp-12-2541-2012, 2012.
8

9 Reinhardt, A., and Doye, J. P. K.: Effects of surface interactions on heterogeneous ice nucleation for a
10 monatomic water model, *Journal of Chemical Physics*, 141, 10.1063/1.4892804, 2014.
11

12 Riechers, B., Wittbracht, F., Hütten, A., and Koop, T.: The homogeneous ice nucleation rate of water
13 droplets produced in a microfluidic device and the role of temperature uncertainty, *Phys. Chem.*
14 *Chem. Phys.*, 15, 5873-5887, 10.1039/C3CP42437E, 2013.
15

16 Slater, B., Michaelides, A., Salzmann, C. G., and Lohmann, U.: A blue-sky approach to understanding
17 cloud formation, *B. Am. Meteorol. Soc.*, 10.1175/bams-d-15-00131.1, 2015.
18

19 Tobo, Y., DeMott, P. J., Hill, T. C. J., Prenni, A. J., Swoboda-Colberg, N. G., Franc, G. D., and
20 Kreidenweis, S. M.: Organic matter matters for ice nuclei of agricultural soil origin, *Atmos. Chem.*
21 *Phys.*, 14, 8521-8531, 10.5194/acp-14-8521-2014, 2014.
22

23 Umo, N. S., Murray, B. J., Baeza-Romero, M. T., Jones, J. M., Lea-Langton, A. R., Malkin, T. L.,
24 O'Sullivan, D., Neve, L., Plane, J. M. C., and Williams, A.: Ice nucleation by combustion ash particles at
25 conditions relevant to mixed-phase clouds, *Atmos. Chem. Phys.*, 15, 5195-5210, 10.5194/acp-15-
26 5195-2015, 2015.
27

28 Vali, G.: Repeatability and randomness in heterogeneous freezing nucleation, *Atmos. Chem. Phys.*, 8,
29 5017-5031, 10.5194/acp-8-5017-2008, 2008.
30

31 Vali, G.: Interpretation of freezing nucleation experiments: Singular and stochastic; sites and
32 surfaces, *Atmos. Chem. Phys.*, 14, 5271-5294, 10.5194/acp-14-5271-2014, 2014.
33

34 Vali, G., DeMott, P., Möhler, O., and Whale, T.: Ice nucleation terminology, *Atmospheric Chemistry*
35 *and Physics Discussions*, 14, 22155-22162, 2014.
36

37 Wenk, H.-R., and Bulakh, A.: *Minerals: Their constitution and origin*, Cambridge University Press,
38 2004.
39

40 Wex, H., DeMott, P. J., Tobo, Y., Hartmann, S., Rösch, M., Clauss, T., Tomsche, L., Niedermeier, D.,
41 and Stratmann, F.: Kaolinite particles as ice nuclei: Learning from the use of different kaolinite
42 samples and different coatings, *Atmos. Chem. Phys.*, 14, 5529-5546, 10.5194/acp-14-5529-2014,
43 2014.

1

2 Whale, T. F., Murray, B. J., O'Sullivan, D., Wilson, T. W., Umo, N. S., Baustian, K. J., Atkinson, J. D.,
3 Workneh, D. A., and Morris, G. J.: A technique for quantifying heterogeneous ice nucleation in
4 microlitre supercooled water droplets, *Atmos. Meas. Tech.*, 8, 2437-2447, 10.5194/amt-8-2437-
5 2015, 2015.

6

7 Wheeler, M. J., Mason, R. H., Steunenberg, K., Wagstaff, M., Chou, C., and Bertram, A. K.: Immersion
8 freezing of supermicron mineral dust particles: Freezing results, testing different schemes for
9 describing ice nucleation, and ice nucleation active site densities, *The Journal of Physical Chemistry*
10 *A*, 119, 4358-4372, 10.1021/jp507875q, 2015.

11

12 Wittke, W., and Sykes, R.: *Rock mechanics*, Springer Berlin, 1990.

13

14 Wright, T. P., and Petters, M. D.: The role of time in heterogeneous freezing nucleation, *J. Geophys.*
15 *Res.-Atmos.*, 118, 3731-3743, 10.1002/jgrd.50365, 2013.

16

17 Wright, T. P., Petters, M. D., Hader, J. D., Morton, T., and Holder, A. L.: Minimal cooling rate
18 dependence of ice nuclei activity in the immersion mode, *J. Geophys. Res.-Atmos.*, 118, 10535-
19 10543, 10.1002/jgrd.50810, 2013.

20

21 Yakobi-Hancock, J. D., Ladino, L. A., and Abbatt, J. P. D.: Feldspar minerals as efficient deposition ice
22 nuclei, *Atmos. Chem. Phys.*, 13, 11175-11185, 10.5194/acp-13-11175-2013, 2013.

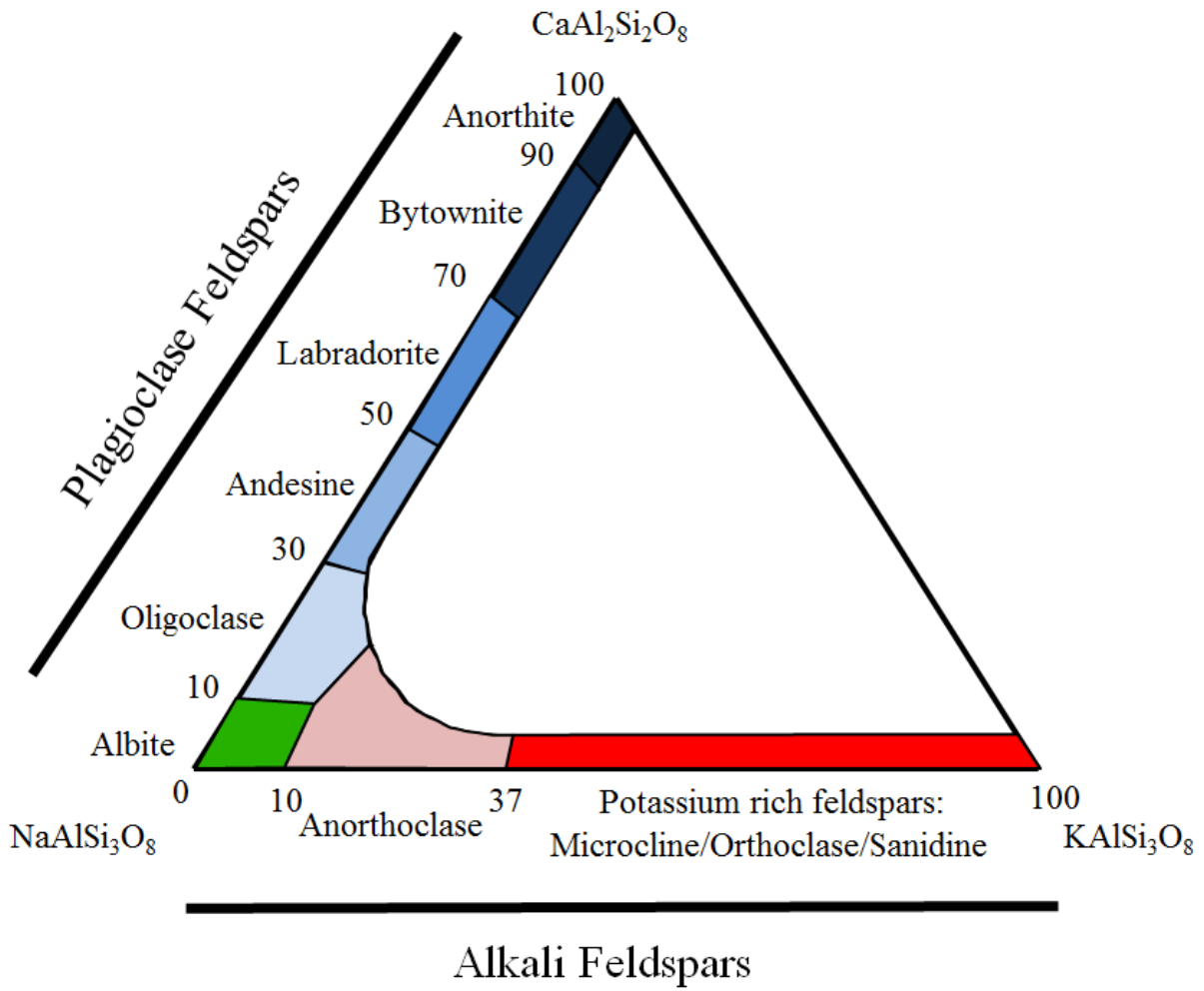
23

24 Zielke, S. A., Bertram, A. K., and Patey, G. N.: Simulations of ice nucleation by kaolinite (001) with
25 rigid and flexible surfaces, *The Journal of Physical Chemistry B*, 10.1021/acs.jpcc.5b09052, 2015.

26

27 Zolles, T., Burkart, J., Häusler, T., Pummer, B., Hitzemberger, R., and Grothe, H.: Identification of ice
28 nucleation active sites on feldspar dust particles, *The Journal of Physical Chemistry A*, 119, 2692-
29 2700, 10.1021/jp509839x, 2015.

1

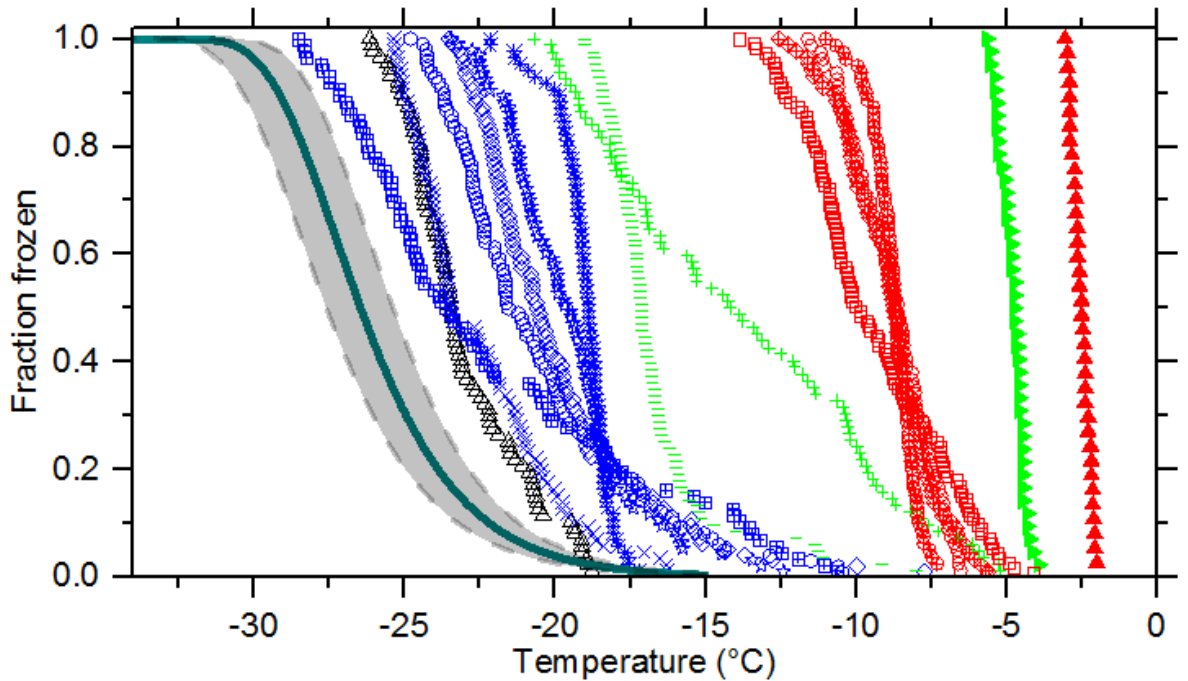


2

3 **Figure 1:** The ternary composition diagram for the feldspars group based on similar figures
4 in the literature (Wittke and Sykes, 1990;Deer et al., 1992).

5

1

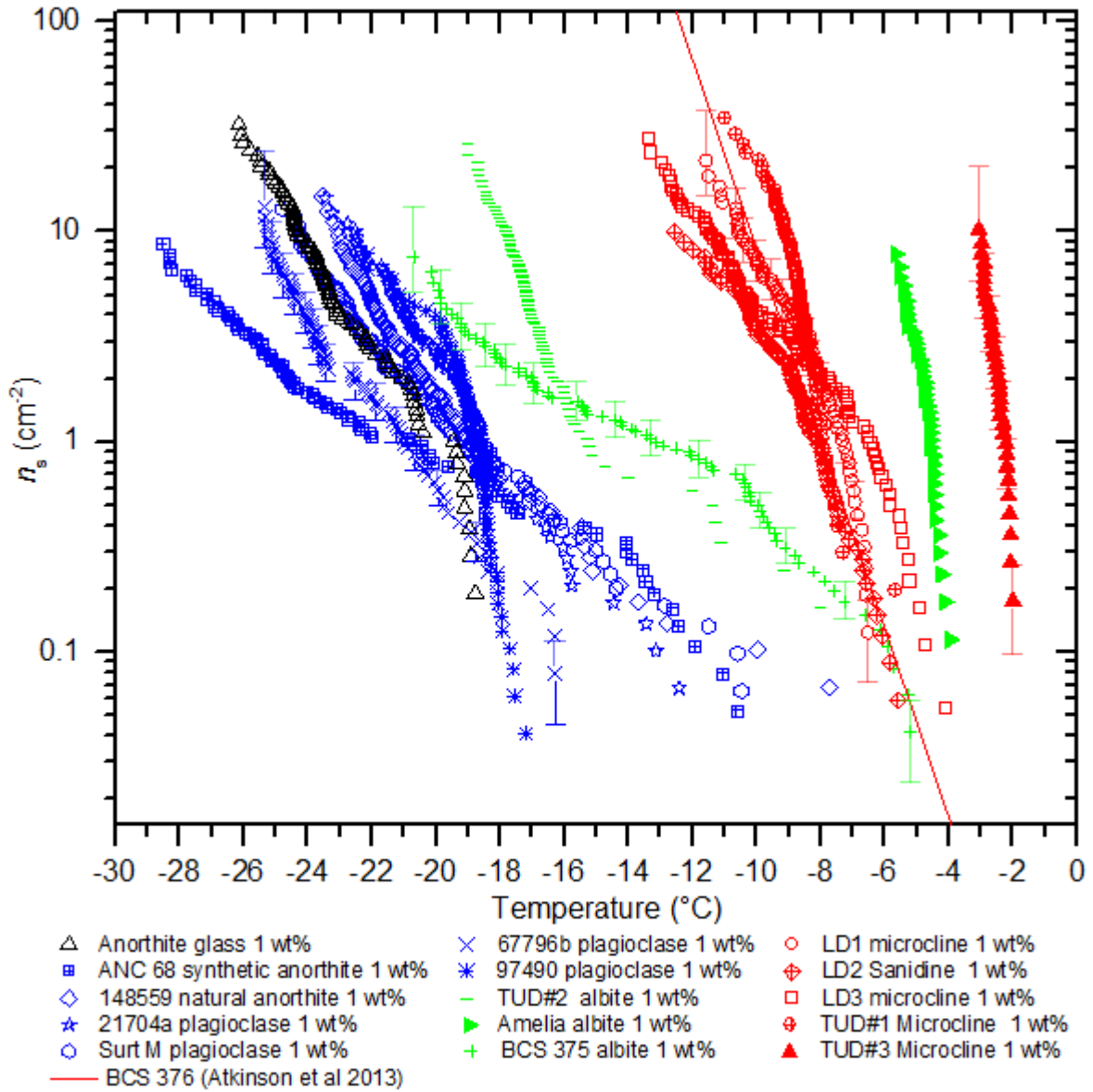


- △ Anorthite glass
- ANC 68 synthetic anorthite
- ◇ 148559 natural anorthite
- ☆ 21704a plagioclase
- Surt M plagioclase
- × 67796b plagioclase
- * 97490 plagioclase
- TUD#2 albite
- ▶ Amelia albite
- + BCS 375 albite
- LD1 microcline
- ◇ LD2 sanidine
- LD3 microcline
- ☆ TUD#1 microcline
- ▲ TUD#3 microcline
- Instrument freezing background

2

3 **Figure 2:** Droplet fraction frozen as a function of temperature for 1 wt% suspensions of
 4 ground powders of various feldspar samples. The K-feldspars are coloured red, the
 5 plagioclase feldspars are coloured blue, the albites are coloured green and the feldspar glass
 6 is coloured black. A fit to the background freezing of pure MilliQ water in the μ l-NIPI
 7 instrument used by Umo et al. (2015) is also included. The shaded area around this fit shows
 8 95% confidence intervals for the fit. It can be seen that all the feldspar samples tested
 9 nucleate ice more efficiently than the background freezing of the instrument.

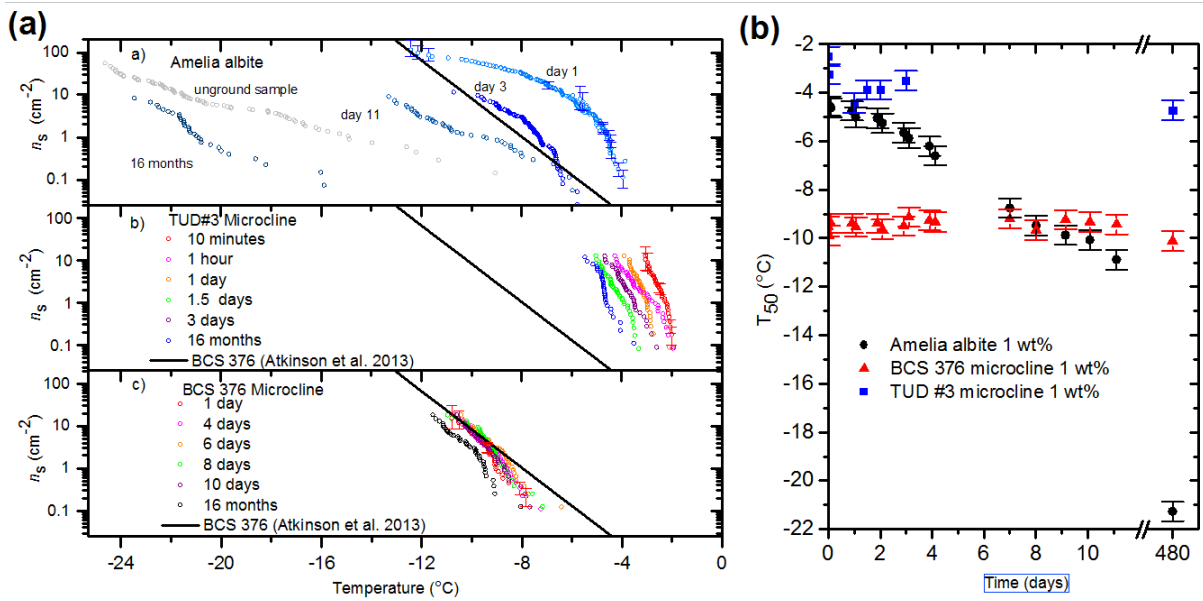
10



1

2 **Figure 3:** Ice nucleation efficiency expressed as $n_s(T)$ for the various feldspars tested in this
 3 study. The K-feldspars are coloured red, the plagioclase feldspars are coloured blue, the
 4 albites are coloured green and the feldspar glass is coloured black. Except for Amelia albite
 5 and TUD#1 microcline all samples were tested twice and the data from the two runs
 6 combined. Sample information can be found in tables 1 and 2. Temperature uncertainty is
 7 $\pm 0.4^{\circ}\text{C}$. Y-Error bars calculated using the Poisson Monte Carlo procedure described in Sect.
 8 4. Data points with large uncertainties greater than an order of magnitude have been removed,
 9 these are invariably the first one or two freezing events of a given experiment. For clarity
 10 error bars have only been included on a selection of datasets (TUD#3 microcline, LD1
 11 microcline, BCS 375 albite and 67796b plagioclase). The error bars shown are typical.

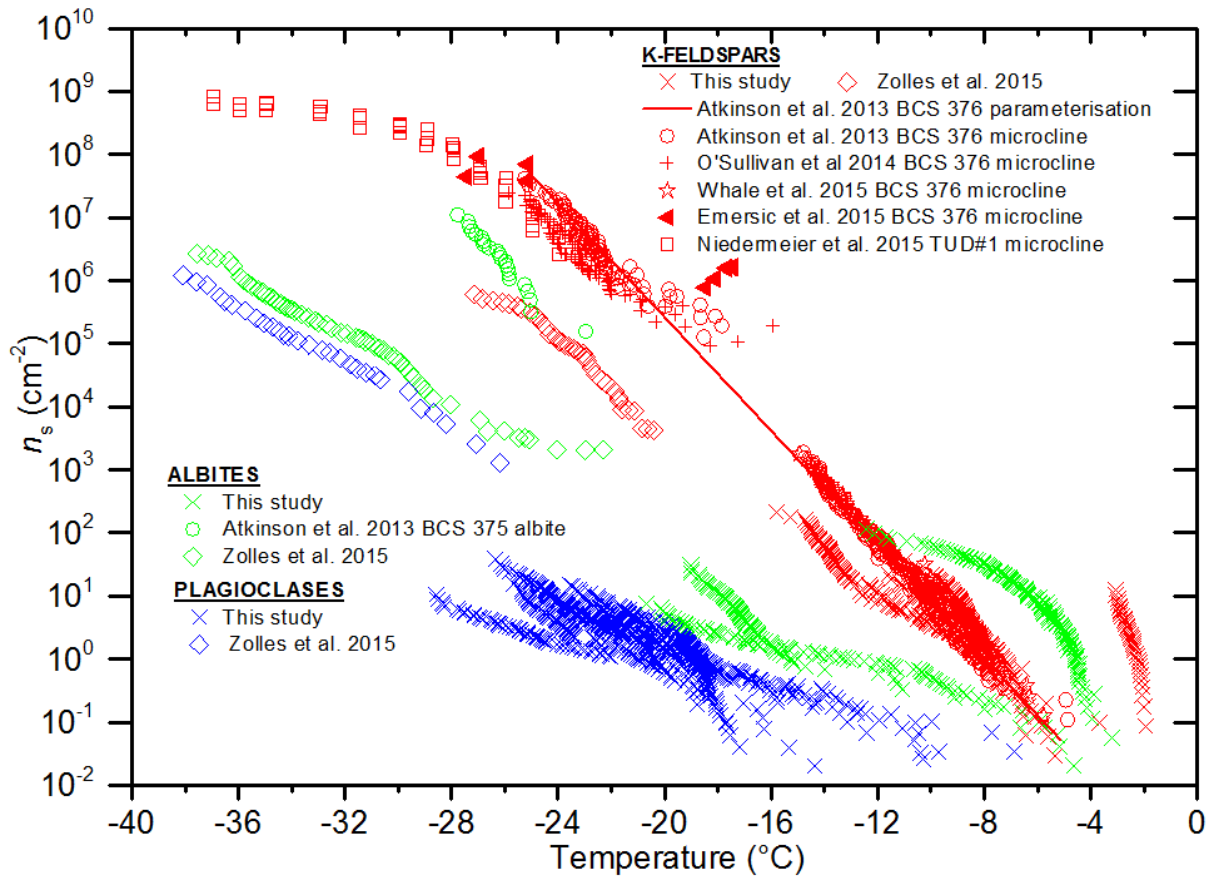
12



1

2 **Figure 4:** (a) The dependence of n_s on time spent in water for three feldspar samples. The
 3 time periods indicate how long samples were left in contact with water. Fresh samples were
 4 tested minutes after preparation of suspensions. Note that ice nucleation temperatures of BCS
 5 376 are almost the same after 16 months in water while those of Amelia albite decreases by
 6 around 16°C. TUD #3 microcline loses activity quickly in the first couple of days of exposure
 7 to water but total decrease in nucleation temperatures after 16 months is only around 2°C. (b)
 8 Median freezing temperature against time left in suspension for BCS 376 microcline, TUD#3
 9 microcline and Amelia albite.

10



1

2 **Figure 5:** Comparison of literature data from Atkinson et al. (2013), Emersic et al. (2015),
 3 Niedermeier et al. (2015) and Zolles et al. (2015) with data from this study. Feldspars are
 4 coloured according to their composition, as in Figure 3. 0.1 wt% data for Amelia albite and
 5 LD1 microcline, which is not shown in figure 3, has been included. Where samples are
 6 known to lose activity with time the most active runs have been shown. Note that data from
 7 Niedermeier et al. (2015) includes some data from Augustin-Bauditz et al. (2014).

8

9

10

11

12

13

14

15

16

17

1 Table 1. Plagioclase feldspars used in this study.

2

Sample	Composition*	Source location	Source of composition/phase data	Space group	Point group	Crystal system
Anorthite glass	An ₁₀₀	Synthetic sample	(Carpenter, 1991)	-	-	-
ANC 68	An ₁₀₀	Synthetic sample	(Carpenter, 1991) describes similar feldspars	P $\bar{1}$	$\bar{1}$	triclinic
148559	An _{99.5} Ab _{0.5}	University of Cambridge mineral collection	-----	P $\bar{1}$	$\bar{1}$	triclinic
21704a	An ₈₆ Ab ₁₄	Viakfontein, Bushveld complex, Transvaal (Harker collection no. 21704)	(Carpenter et al., 1985)	P $\bar{1}$ - $\bar{1}$	$\bar{1}$	triclinic
Surt M	An ₆₄ Ab ₃₆	Surtsey (no. 7517, Iceland Natural History Museum) Phenocrysts from volcanic ejecta	(Carpenter, 1986)	C $\bar{1}$	$\bar{1}$	triclinic
67796b	An ₆₀ Or ₁ Ab ₃₉	Gulela Hills, Tanzania (Harker collection no. 67796)	(Carpenter et al., 1985)	Incommensurate order	-	triclinic
97490	An ₂₇ Or ₁ Ab ₇₁	Head of Little Rock Creek, Mitchell co., N. Carolina (P. Gay, U.S.N.M. no. 97490)	(Carpenter et al., 1985)	Incommensurate order	-	triclinic

3

4 *This refers to the chemical makeup of the feldspars. An stands for anorthite, the calcium end-
 5 member, Ab stands for albite, the sodium end-member and Or stands for orthoclase, the potassium
 6 end-member.

7

1 Table 2. Alkali feldspars used in this study.

Sample	Dominant feldspar phase	Source location	Source of composition/phase data	Space group	Point group	Crystal system
LD1 microcline	microcline	University of Leeds rock collection	XRD	$C\bar{1}$	$\bar{1}$	triclinic
LD2 sanidine	sanidine	University of Leeds rock collection	XRD	$C2/m$	$2/m$	monoclinic
LD3 microcline	microcline	University of Leeds rock collection	XRD	$C\bar{1}$	$\bar{1}$	triclinic
BCS 376 microcline	microcline	Bureau of Analysed Samples Ltd	Reference sample/XRD (Atkinson et al., 2013)	$C\bar{1}$	$\bar{1}$	triclinic
Amelia Albite (un-ground)	albite	Amelia Courthouse, Amelia Co., Virginia (Harker mineral collection)	(Carpenter et al., 1985)	$C\bar{1}$	$\bar{1}$	triclinic
Amelia Albite ground	albite	Amelia Courthouse, Amelia Co., Virginia (Harker mineral collection)	(Carpenter et al., 1985)	$C\bar{1}$	$\bar{1}$	triclinic
TUD#1 microcline	microcline	Minas Gerais, Brazil	XRD	$C\bar{1}$	$\bar{1}$	triclinic
TUD#2 albite	albite*	Norway	XRD	$C\bar{1}$	$\bar{1}$	triclinic
TUD#3 microcline	microcline	Mt. Maloso, Malawi	XRD	$C\bar{1}$	$\bar{1}$	triclinic
BCS 375 albite	albite	Bureau of Analysed Samples Ltd	Reference sample/XRD (Atkinson et al., 2013)	$C\bar{1}$	$\bar{1}$	triclinic

2 * We note that the XRD pattern was also consistent with oligoclase, which is close to albite in
3 composition. The identification of albite is consistent with that of Alexei Kiselev (Personal
4 communication).